Original Article

High-resolution reduced field-of-view diffusion-weighted magnetic resonance imaging in the diagnosis of cervical cancer

Lijuan Mao[1], Xiaoling Zhang[1], Tingting Chen[2], Zhoulei Li[1], Jianyong Yang[1]^

[1]Department of Medical Imaging, The First Affiliated Hospital, Sun Yat-sen University, Guangzhou, China; [2]Xin Hua College of Sun Yat-sen University, Guangzhou, China

Contributions: (I) Conception and design: L Mao, J Yang; (II) Administrative support: L Mao, J Yang; (III) Provision of study materials or patients: L Mao, X Zhang, Z Li; (IV) Collection and assembly of data: L Mao, X Zhang, T Chen, Z Li; (V) Data analysis and interpretation: X Zhang, T Chen; (VI) Manuscript writing: All authors; (VII) Final approval of manuscript: All authors.

Correspondence to: Jianyong Yang; Xiaoling Zhang. Department of Medical Imaging, The First Affiliated Hospital, Sun Yat-sen University, No. 58, Guangzhou 510080, China. Email: dryangjianyong@126.com; lindarzhang@126.com.

Background: Magnetic resonance imaging (MRI) has now become the best modality for the preoperative staging of cervical cancer. This study was to compare the value of high-resolution reduced field-of-view diffusion-weighted MR imaging (r-FOV DWI) with conventional field-of-view (c-FOV DWI) in the diagnosis of cervical cancer.

Methods: Forty-five patients (25 patients with cervical cancer and 20 patients with normal cervix) received magnetic resonance (MR) scans (3.0T), including both r-FOV DWI and c-FOV DWI sequences. The image quality (IQ) of both sequences was subjectively assessed by two attending radiologists using a double-blind method and quantitatively by the signal-to-noise ratio (SNR) and contrast-to-noise ratio (CNR). Moreover, apparent diffusion coefficient (ADC) values for cervical cancer were blindly measured by one technician on the ADC map.

Results: The subjective scores of r-FOV DWI images were higher than those of c-FOV DWI (P<0.0001), and the interrater reliability was in good agreement [Cohen's kappa coefficient (κ) =0.547–0.914]. There was a significant difference in CNR between the two DWI image groups (r-FOV DWI 12.73±5.56 *vs.* c-FOV DWI 11.21±5.92, P=0.019). The difference in mean ADC values between the two DWI sequences was statistically significant [r-FOV DWI (0.690±0.195)×10^{-3} mm^2/s *vs.* c-FOV DWI (0.794±0.167)×10^{-3} mm^2/s, P<0.001]. The ADC value of cervical cancer lesions [(0.690±0.195)×10^{-3} mm^2/s] was significantly lower than that of normal cervix ADC value [(1.506±0.188)×10^{-3} mm^2/s].

Conclusions: r-FOV DWI can effectively improve the spatial resolution of the image while reducing distortion and artifacts. Furthermore, it can help to diagnose cervical cancer more accurately for the more realistic ADC values.

Keywords: Diffusion-weighted MR imaging (DWI); reduced field-of-view; high-spatial-resolution; cervical cancer

Submitted Jun 09, 2022. Accepted for publication Mar 01, 2023. Published online Mar 20, 2023.
doi: 10.21037/qims-22-579
View this article at: https://dx.doi.org/10.21037/qims-22-579

^ ORCID: 0000-0002-8110-3188.

Introduction

Currently, cervical cancer has become the fourth most common cancer among women in the world. According to the GLOBOCAN 2020 database of the International Agency for Research on Cancer (IARC), approximately 604,000 women have been diagnosed with cervical cancer in 2020. Cervical cancer tends to evolve from years of precancerous or high-grade lesions (1). Therefore, early identification and treatment of cervical cancer can result in a very high cure and survival rate, hence early screening of cervical lesions is critical (2). Magnetic resonance imaging (MRI) has now become the single best modality for the preoperative staging of cervical cancer. It plays an important role in the initial assessment of patients, from the extent of disease to treatment options and follow-up efficacy, and its superior soft tissue resolution improves Federation International of Gynecology and Obstetrics (FIGO) clinical staging accuracy and makes treatment options more reasonable (3).

Diffusion-weighted MR imaging (DWI) utilizes Brownian motion or free diffusion phenomena in water molecules to provide a non-invasive means of detecting the restricted diffusion motion of water molecules *in vivo* (4). In a completely unrestricted environment, the motion of water molecules is completely random. However, due to tissue morphology, physiology, and pathology, water molecular movement in human tissues is not completely random, and tissue types such as tumors, cytotoxic edema, abscess, and fibrosis all appear as dispersion restrictions (5). Thus, DWI can reflect cytopathic lesions by the motion of water molecules, and tumors appear as high signal on high b value images, exhibits dispersion restriction on apparent diffusion coefficient (ADC) graphs, and ADC values decrease, that can be distinguished from normal tissues. Currently, the single-shot echo-planar imaging (SS-EPI) sequence obtains the entire k space after a single excitation pulse, and the image is not subject to shadow effects from motion-induced phase errors. However, its long readout times during T2* attenuation result in a severely blurred image along the phase-encode direction; on the other hand, the interval between the K space profiles is long due to the polarization effect causing deformation and artifacts (6). SS-EPI technology is used for conventional field-of-view (c-FOV DWI) imaging, when SS-EPI and DWI are combined to further increase resolution without pronounced geometric distortion, the resulting images are often corrupted by a high level of noise and artifact due to the numerical restriction in sensitivity encoding, and the zonal oblique multislice Echo-Planar Imaging (ZOOM-EPI) technology is used for high-resolution reduced field-of-view diffusion-weighted MR imaging (r-FOV DWI), which can significantly improve image quality (IQ) and significantly reduce image distortion and magnetic sensitivity artifacts (7).

In recent years, with technological development, two-dimensional spatially selective radiofrequency pulses (2D RF) and 180 reunion pulse techniques have been applied for r-FOV imaging. 2D RF consists of an RF pulse along the horizontally selected direction and RF pulses along the PE direction while exciting a certain thickness of the level, thus reducing the field of view and PE step length along the PE direction while shortening the EPI echo chain and echo duration without increasing the scan time. Compared with conventional SS-EPI sequences, r-FOV imaging techniques reduce image deformation and magnetically sensitive artifacts and improve image spatial resolution. In SS-EPI, the k space is sampled line by line by a signal generated by a single 90-degree RF excitation pulse, while the combination of 2D RF and 180 reunion pulses allows multi-layer imaging while suppressing the fat signal (8,9). ZOOM-EPI with r-FOV imaging involves selecting the target level using a 90 RF pulse, followed by oblique plane excitation with a 180 reunion pulse, where the 180 reunion pulse is not parallel to the 90 RF pulse, but at an angle to reduce the field of view (10-12).

A number of studies confirmed that the application of small vision dispersion weighted image technology can significantly improve IQ, significantly reduce image deformation and magnetic sensitive artifacts in the kidney (11), spinal cord (13), brain (14), nerve (15), neck (16), prostate (17), pancreas (18,19), uterus (20-22), breast (23), rectum (12,24), thyroid parts (25). These will improve the doctor's diagnosis confidence, and even help to improve the accuracy of tumor staging.

At present, the research on r-FOV imaging technology in cervical cancer has not been very perfect (20,22). Colposcopy-guided biopsy is used to diagnose cervical cancer and precancerous lesions, which are then staged according to the FIGO staging criteria (26). The FIGO authorized imaging and pathologic findings (if any) to be used in staging in 2018 (27). In the preoperative staging of cervical cancer, MRI has been demonstrated to be extremely accurate (28). As a result, MRI is the preferred method for local staging, assessing therapy response, detecting tumor recurrence, and monitoring cervical cancer patients (29). The primary goal of an MRI scan is to detect peritumoral infiltration and lymph node metastasis (LNM) (30). Wang

Table 1 r-FOV DWI and c-FOV DWI sequence imaging parameters

Sequence parameters	r-FOV	c-FOV
TR/TE (msec)	4,916/99	4,106/76
FOV (mm)	130×101×72	240×240×101
Matrix (mm)	72×58	120×118
Pixel resolution (mm)	0.81×0.81	1.88×1.88
Slice thickness (mm)	3	4
No. of slice	24	23
NEX	2	1
b value (sec/mm^2)	0/1,000	0/1,000
Flip angle (°)	90	90
BW (Hz)	1,727	2,384

r-FOV DWI, reduced field-of-view diffusion-weighted MR imaging; c-FOV DWI, conventional field-of-view diffusion-weighted MR imaging; TR/TE, the repetition time/the echo time; FOV, field-of-view; NEX, number of excitations; BW, bandwidth.

et al. found that T2WI and DWI-based radiography images had a high prediction power for pelvic LNM in early cervical cancer (31).

FIGO stage IVA uterine cervical carcinoma with bladder mucosal invasion is associated with a poor prognosis. Although MRI can rule out bladder invasion and avoid cystoscopy, the significant false-positive rate can be troublesome. Takeuchi *et al.* reported that in 13 of the 15 instances, cystoscopy confirmed mucosal invasion. In all 15 cases, the border between the tumor and the bladder wall was vague on T2WI but obvious on r-FOV DWI. The diagnosis of mucosal invasion on r-FOV DWI exhibited the sensitivity of 100%, the specificity of 50%, the accuracy of 93%, the positive predictive value of 93%, and the negative predictive value of 100% (32). The r-FOV DWI sequence outperformed the full field-of-view DWI sequence in terms of IQ and lesion visibility. Furthermore, r-FOV sequences can be utilized to assess FIGO cervical cancer staging (33). The aim of this study was to compare the value of c-FOV DWI and r-FOV DWI in cervical cancer diagnosis by qualitative analysis of IQ and quantitative analysis of ADC.

Methods

Ethical statement

The study was conducted in accordance with the Declaration of Helsinki (as revised in 2013). The study was approved by the Ethics Committee of Sun Yat-sen University (ID of the approval: 2020-536). All patients signed an informed consent form before the MR examination was performed. Informed consent was obtained from each patient for this study analysis.

Population

Forty-nine patients with cervical cancer who underwent MRI between October 2020 and April 2021 were collected. Inclusion criteria for patients with cervical cancer: (I) patients with cervical cancer confirmed by surgical resection or puncture biopsy; (II) all patients had preoperative MRI; (III) none of the patients had undergone other invasive procedures on the uterus or cervix. Exclusion criteria: (I) history of conization or loop electrosurgical excision procedure (LEEP) before MRI; (II) chemotherapy or radiotherapy before MRI; (III) poor IQ in severe distortion in some patients due to the effect of bowel contents. Of these excluded patients, 12 patients underwent conization or LEEP, 8 patients underwent radiotherapy before the examination, and 4 patients with poor IQ of MR examination results. The remaining 25 patients with cervical cancer (age 28–77 years, mean age 53.76±11.39 years) were finally included.

Twenty age-matched women with non-cervical lesions were set up as controls (age range 26–64 years, mean age 47.15±10.52 years). Their inclusion criteria: (I) pelvic uterine MRI for other reasons; (II) no previous uterine or cervical lesions and no uterine or cervical treatment. Exclusion criteria: (I) history of uterine or cervical pathology or individuals who have undergone interventional diagnostic or therapeutic procedures on the uterus or cervix; (II) the patient's MRI was severely distorted by the intestinal contents.

Magnetic resonance examinations

All patients received a 3.0T MRI scan (Ingenia CX 3.0T; Philips Medical System, Best, The Netherlands) using a digital RF receiver coil with a 16-element phased array. The patient was lying on an examination bed with the foot extended forward and the pubococcygeal joint positioned at a center of 5 cm (34). There are still no uniform criteria for intestinal preparation before cervical MRI (20). Thus, no intestinal preparation was performed. The scanning sequence includes r-FOV DWI and c-FOV DWI. The imaging parameters for both sequences were as follows (*Table 1*).

Table 2 Evaluation criteria of image quality with the quarter-point method

Rating items	1	2	3	4
Image anatomy details	Unrecognized	Indistinct	Clear profile and fuzzy edges	Clear profile and clear edges
Image sharpness	Un-sharpness	Slightly sharper	Sharper	Sharp
Image geometric deformation	Unrecognizable lesion	Inconsistent with the anatomical sequence image profile	Consistent slightly with the anatomical sequence image profile	Consistent with the anatomical sequence image profile
Ghost shadows, motion, and magnetically sensitive artifacts	Serious	Obvious	Slight	Few or none
Lesion significance	Fail to identify	Identifiable	Fuzzy edge	Clear edges
Overall image quality	Unable to diagnose	Has a certain impact on the diagnosis	Basic satisfied diagnosis	Good for the diagnosis

Image analysis

Qualitative analyses

Images of cervical cancer patients from c-FOV DWI and r-FOV DWI sequences with a b value of 1,000 s/mm^2 were selected and evaluated by two radiologists in a double-blind manner. The evaluation included anatomical details, image clarity, image geometric distortion, artifacts, lesion significance, and IQ of both DWI sequences using a 4-point scale (12,20,22) as shown in *Table 2*.

Quantitative analyses

Signal-to-noise ratio (SNR) and contrast-to-noise ratio (CNR)

SNR and CNR was measured by technicians at the Philips post-processing workstation (IntelliSpace Portal, version 9.0), and regions of interest were manually outlined on images with 1,000 s/mm^2 b values of c-FOV DWI sequences and r-FOV DWI sequences, respectively, using the measurement tools of the post-processing workstation. A circular region of interest (ROI) was used, and the largest level of the cervical lesion was selected as a reference for the T2WI level fracture image, and three ROIs were randomly outlined to avoid necrosis, signal inhomogeneity, and artifact areas, with an ROI size of approximately 10 mm^2 (9.7–10.3 mm^2). The signal mean and standard deviation of each ROI were taken, and the mean of the three values was calculated. Meanwhile, normal muscle tissue (gluteus maximus) signals were measured at the same image level in all patients, the signal mean and standard deviation of each ROI were taken, and the average of the three was calculated (11,12,20,22).

SNR (Eq. [1]) is defined as the percentage between the mean signal intensity inside the tumor (Stumor) and the standard deviation (SD) of background noise. CNR (Eq. [2]) is a measure used to determine IQ, where S_{tumor} and S_{tissue} are signal intensities for signal-producing tumor and tissue in the ROI and σ_o is the standard deviation of the pure image noise (SD_{air}). The formula is shown below (24):

$$SNR = \frac{S_{tumor}}{SD_{background}} \quad [1]$$

$$CNR = \frac{\left|S_{tumor} - S_{tissue}\right|}{\sigma_o} \quad [2]$$

ADC values

At the post-processing workstation, technicians blindly measured the ADC values, and the ROI outlined on the image with a b value of 1,000 s/mm^2 was copied to the corresponding ADC map to ensure that the ADC diagram matched the ROI region with a b value of 1,000 s/mm^2, and the average of the three ROIs were taken after the measurement. *Figure 1* depicts the ROI outline standard reference.

Statistical analyses

All statistical analyses were performed using SPSS v.23.0 (IBM SPSS Statistics, Armonk, NY, USA), and P<0.05 has statistical significance. The images were assessed by two independent readers, and Cohen's Kappa coefficient (κ) was used to determine intra-rater reliability. The paired Wilcoxon symbolic rank-sum test was used to compare the qualitative picture quality scores of r-FOV DWI sequences and c-FOV DWI sequences. The paired Wilcoxon symbolic

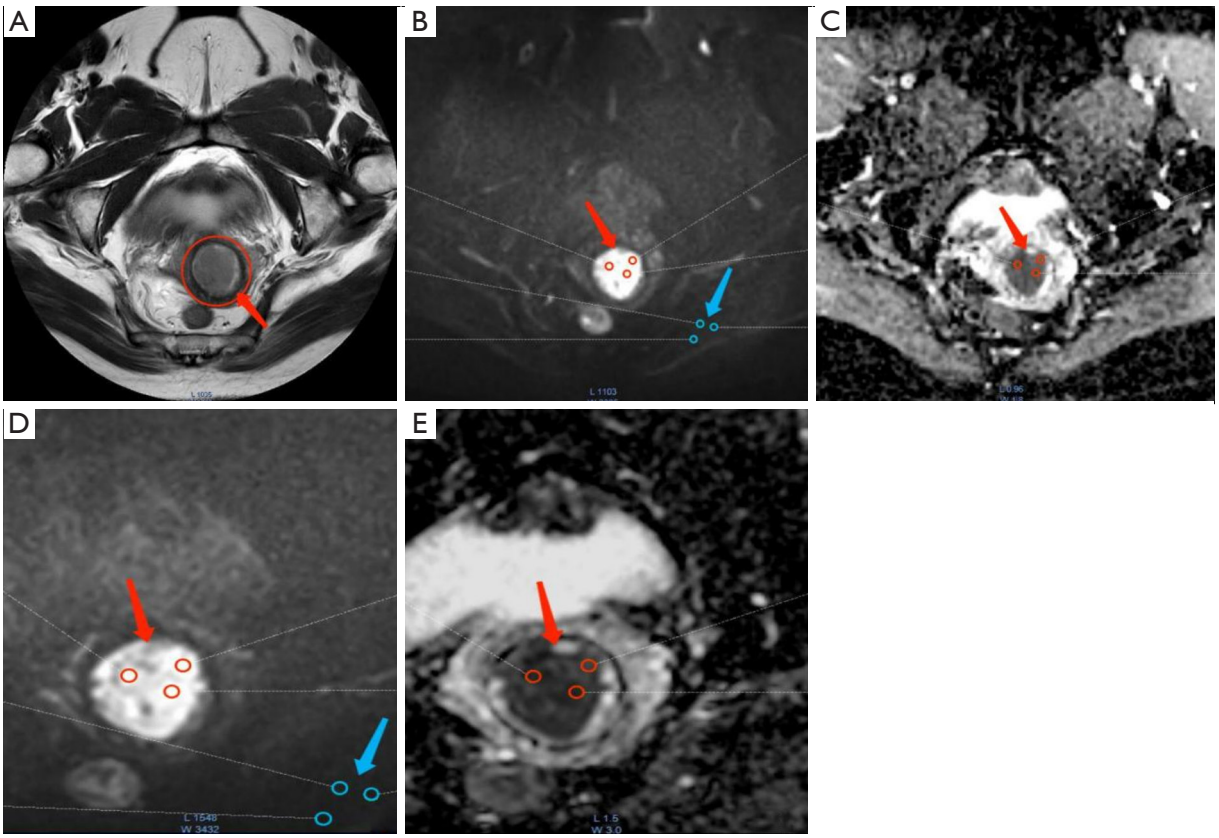

Figure 1 Reference diagrams of measured values of ROI outline standards. (A) Reference diagrams of T2WI horizontal break sites for the T2WI_MVXD_TRA sequence, with red arrow indicating lesions. (B) High b value (b=1,000 s/mm^2) diagram of the c-FOV DWI sequence, with red arrow indicating three random ROIs at the lesion and blue arrow indicating three random ROIs in the normal muscle tissue (gluteus maximus). (C) ADC plot of c-FOV DWI sequence, red arrow indicates three random ROIs at the lesion. (D) High b value (b=1,000 s/mm^2) plot of r-FOV DWI sequence, red arrow indicates three random ROIs at the lesion and blue arrow indicates three random ROIs in the normal muscle tissue (gluteus maximus). (E) ADC plot of r-FOV DWI sequence, red arrow indicates three random ROIs at the lesion. ROI, region of interest; T2WI, T2 weighted image; MVXD, MultiVane-XD; c-FOV DWI, conventional field-of-view diffusion-weighted MR imaging; ADC, apparent diffusion coefficient; r-FOV, reduced field-of-view.

Table 3 Age comparison results of cervical cancer and normal control groups

Groups	Number	Mean ± SD (years)	P
Cervical cancer	25	53.76±11.38	0.052
Normal control	20	47.15±10.52	

rank-sum test was used to compare the SNR and CNR of picture quality for r-FOV DWI and c-FOV DWI in the cervical cancer group. The results were presented as mean ± SD. Normal distribution and homogeneity of variance were assessed by the Kruskal-Wallis test. The independent sample *t*-test was used to compare statistical differences in age between cervical cancer and normal control groups and the ADC differences (ROI) between r-FOV DWI and c-FOV DWI sequences in the cervical cancer group, as well as the ADC differences between cervical and normal groups in the r-FOV DWI sequence.

Results

Comparison of baseline data

Independent samples *t*-test comparing the age divergence between the cervical cancer group and the normal control group disclosed no statistically significant (t=2.001, P>0.05, *Table 3*).

Table 4 Consistency test of qualitative image quality scores by radiologists

Sequences	Evaluating indicator	Kappa	P
r-FOV DWI	Image anatomy details	0.815	<0.001
	Image sharpness	0.682	<0.001
	Image geometric deformation	0.675	<0.001
	Ghost shadows, motion, and magnetically sensitive artifacts	0.914	<0.001
	Lesion significance	0.684	<0.001
	Overall image quality	0.891	<0.001
c-FOV DWI	Image anatomy details	0.583	<0.001
	Image sharpness	0.561	<0.001
	Image geometric deformation	0.833	<0.001
	Ghost shadows, motion, and magnetically sensitive artifacts	0.547	<0.001
	Lesion significance	0.592	<0.001
	Image geometric	0.594	<0.001

r-FOV DWI, reduced field-of-view diffusion-weighted MR imaging; c-FOV DWI, conventional field-of-view diffusion-weighted MR imaging.

Table 5 Qualitative image quality scores for the r-FOV DWI and c-FOV DWI sequences and comparison results of SNR and CNR in the cancer group

Evaluating indicators	r-FOV DWI	c-FOV DWI	P
Image anatomy details	3.78±0.62	2.90±0.54	<0.001
Image sharpness	3.80±0.57	2.90±0.54	<0.001
Image geometric deformation	3.84±0.42	3.58±0.50	<0.005
Ghost shadows, motion, and magnetically sensitive artifacts	3.62±0.60	3.22±0.65	<0.001
Lesion significance	3.58±0.86	2.86±0.76	<0.001
Overall image quality	3.66±0.69	2.86±0.61	<0.001
SNR	16.29±6.09	17.66±9.23	0.946
CNR	12.73±5.56	11.21±5.92	0.019

r-FOV DWI, reduced field-of-view diffusion-weighted MR imaging; c-FOV DWI, conventional field-of-view diffusion-weighted MR imaging; SNR, signal-to-noise ratio; CNR, contrast-to-noise ratio.

Scoring agreement tests between two radiologists

The IQ scores for both sequences of r-FOV DWI and c-FOV DWI were moderate to strong: (I) image anatomy details: r-FOV DWI κ=0.815, c-FOV DWI κ=0.583; (II) image sharpness: r-FOV DWI κ=0.682, c-FOV DWI κ=0.561; (III) image geometric deformation: r-FOV DWI κ=0.675, c-FOV DWI κ=0.833; (IV) ghost shadows, motion, and magnetically sensitive artifacts: r-FOV DWI κ=0.914, c-FOV DWI κ=0.547; (V) lesion significance: r-FOV DWI κ=0.684, c-FOV DWI κ=0.592; (VI) image geometric: r-FOV DWI κ=0.891, c-FOV DWI κ=0.594 (*Table 4*). Cohen's kappa results showed moderate to almost perfect agreement (κ values between 0.547 and 0.914).

Qualitative IQ score comparison

The qualitative IQ scoring results for the r-FOV DWI and c-FOV DWI sequences were shown in *Table 5*. In the evaluation of IQ by two radiologists, DWI sequences with r-FOV achieved significantly better scores than

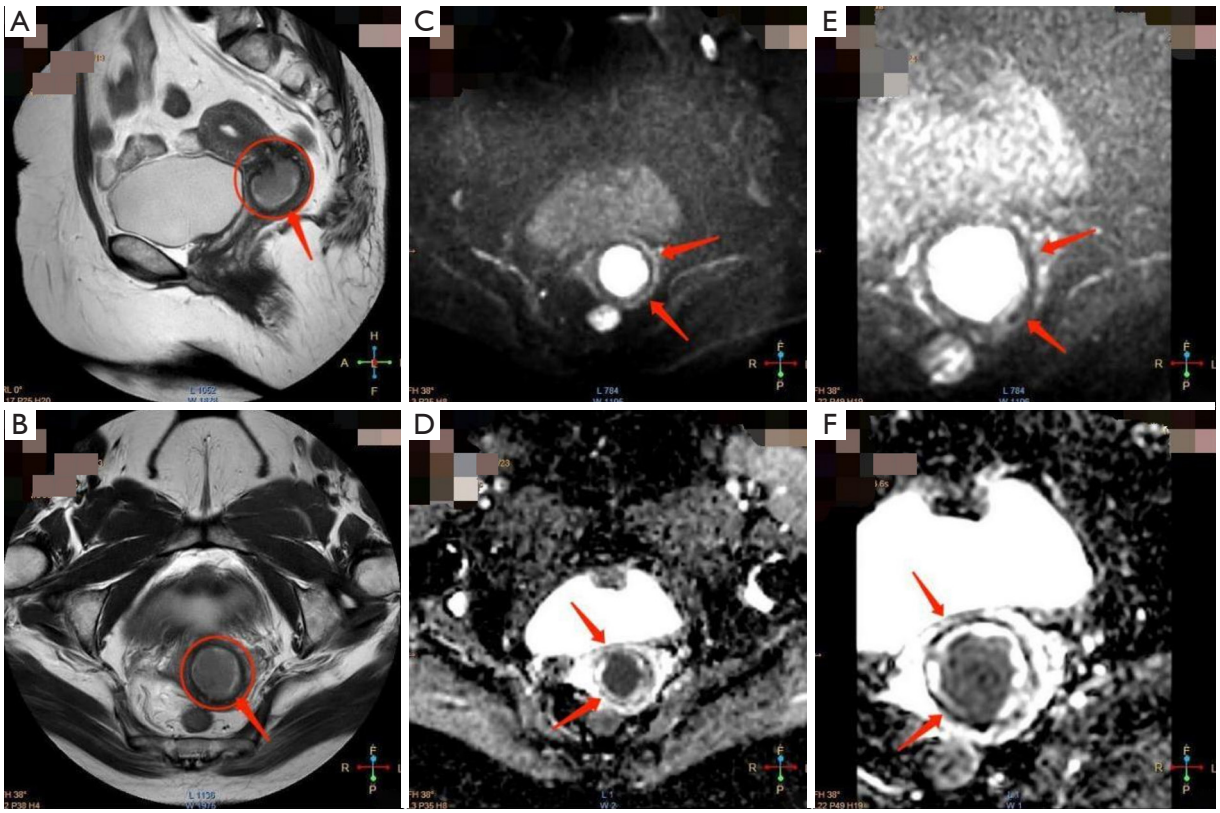

Figure 2 FIGO staging of a 61-year-old woman with stage IB2 cervical adenocarcinoma. (A) Sagittal T2WI image. (B) Transverse T2WI image. (C) c-FOV DWI high b value map (b=1,000 s/mm^2). (D) c-FOV DWI ADC diagram. (E) r-FOV DWI high b value diagram (b=1,000 s/mm^2). (F) r-FOV DWI ADC diagram. A cervical circular mass shadow is visible on the T2WI image (indicated by the red arrow), where a higher signal is shown. Comparing the high b values and ADC maps of the two sequences (indicated by the red arrow), the r-FOV DWI shows more anatomical details, and the edges of the lesion are more clearly defined. FIGO, Federation International of Gynecology and Obstetrics; T2WI, T2 weighted image; c-FOV DWI, conventional field-of-view diffusion-weighted MR imaging; r-FOV DWI, reduced field-of-view diffusion-weighted MR imaging; ADC, apparent diffusion coefficient.

the conventional DWI sequence in image anatomical details, image sharpness, image geometry deformation, ghost, motion, and magnetically sensitive artifacts, lesion significance, and overall IQ (*Figures 2,3*). The following six metrics were compared: anatomical details in the image, where r-FOV DWI scored 3.78±0.62 and c-FOV DWI scored 2.90±0.54 (P<0.001); image sharpness, where r-FOV DWI scored 3.80±0.57 and c-FOV DWI scored 2.90±0.54 (P<0.001); image geometry deformation, where r-FOV DWI scored 3.84±0.42 and c-FOV DWI scored 3.58±0.50 (P<0.05); ghost, motion, and magnetically sensitive artifacts, where r-FOV DWI scored 3.62±0.60 and c-FOV DWI scored 3.22±0.65 (P<0.001); lesion significance, where r-FOV DWI scored 3.58±0.86 and c-FOV DWI scored 2.86±0.76 (P<0.001); and overall IQ, where r-FOV DWI scored 3.66±0.69 and c-FOV DWI scored 2.86±0.61 (P<0.001).

Comparisons of SNR and CNR

There was no statistically significant difference between the two sequences of r-FOV DWI and c-FOV DWI in the cervical cancer group (r-FOV DWI 16.29±6.09 *vs.* c-FOV DWI 17.66±9.23, P=0.946). Comparing the CNR ratios of the two sequences, the difference was statistically significant (r-FOV DWI 12.73±5.56 *vs.* c-FOV DWI 11.21±5.92, P=0.019, *Table 5*).

Quantitative analyses of the ADC values

By quantitative analysis, the difference in mean ADC values between the two DWI sequences was statistically significant [r-FOV DWI (0.690±0.195)×10^{-3} mm^2/s *vs.* c-FOV DWI (0.794±0.167)×10^{-3} mm^2/s, P<0.001, *Figure 4*]. In the

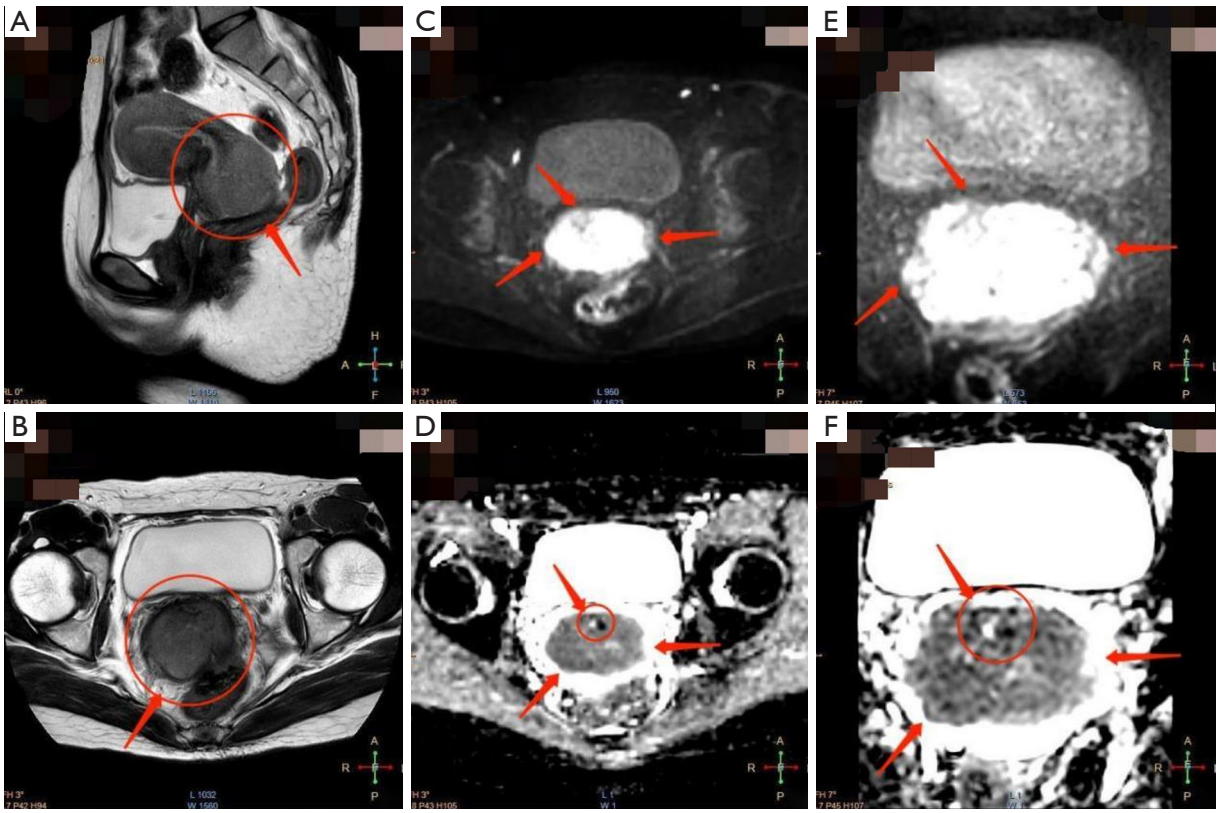

Figure 3 Qualitative image quality score comparison. (A) Sagittal T2WI image. (B) Transverse T2WI image. (C) c-FOV DWI high b value map (b=1,000 s/mm^2). (D) c-FOV DWI ADC map. (E) r-FOV DWI high b value map (b=1,000 s/mm^2). (F) r-FOV DWI ADC map. FIGO staging of a 38-year-old woman with stage IIA2 squamous carcinoma of the cervix. An irregularly shaped soft tissue mass in the cervix (indicated by the red arrow) is seen on the T2WI image with the equivalent signal. Comparing the high b value and ADC maps of the two sequences (indicated by red arrows), the r-FOV DWI shows more anatomical details, with clearer lesion margins and a more detailed inhomogeneous signal. T2WI, T2 weighted image; c-FOV DWI, conventional field-of-view diffusion-weighted MR imaging; r-FOV DWI, reduced field-of-view diffusion-weighted MR imaging; ADC, apparent diffusion coefficient; FIGO, Federation International of Gynecology and Obstetrics.

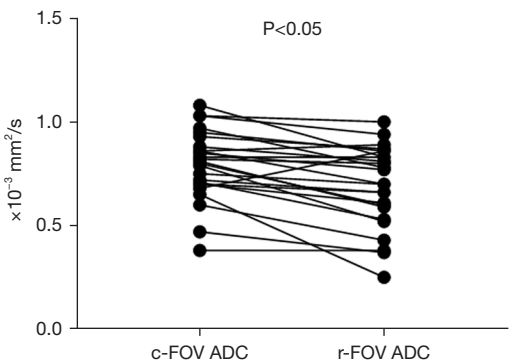

Figure 4 Comparison of r-FOV DWI and c-FOV DWI sequences in the cervical cancer group. ADC, apparent diffusion coefficient; c-FOV DWI, conventional field-of-view diffusion-weighted MR imaging; r-FOV DWI, reduced field-of-view diffusion-weighted MR imaging.

r-FOV DWI sequence, ADC of cervical cancer lesions was significantly lower than that of the normal cervix. The ADC value was (0.690±0.195)×10^{-3} mm^2/s for cervical cancer lesions and (1.506±0.188)×10^{-3} mm^2/s for normal cervix (P<0.05). In the c-FOV DWI sequence, ADC of cervical cancer lesions was significantly lower than that of the normal cervix. The ADC value was (0.794±0.167)×10^{-3} mm^2/s for cervical cancer lesions and (1.394±0.204)×10^{-3} mm^2/s (P<0.05).

Discussion

DWI, as a promising functional imaging technology, plays an important role in the non-invasive detection of the diffusion movement of living water molecules. DWI has

been widely used in MRI. However, full-field DWI with SS-EPI commonly used in clinical practice has problems with low in-plane spatial resolution, obvious anatomical distortion, and magnetic-sensitive artifacts due to rapid acquisition, B0 and B1 field inhomogeneity, and eddy current. Also, the sequence images a wide range of all the anatomy within the pelvis, similar to the MRI of the prostate in men, because the cervix is adjacent to the intestines and the bladder, it is vulnerable to magnetically sensitive artifacts from intestinal gas, feces and filled liquid in the bladder or chemical artifacts, thus the sequence emphasizes the deformation and distortion of the image (17,20,22). Reduced FOV imaging technique with ZOOM-EPI applied the 2D method of a selective excitation pulse to reduce the imaging field along the phase coding direction (9), simply stimulate limited areas of interest, excluding the effects of a portion of the surrounding rectal gas, greatly reduces the distortion and artifacts of the cervical anatomy.

Spatial resolution

Spatial resolution is the resolution of the image to fine anatomical structure, which is one of the important parameters of IQ control in MR. The spatial resolution of the image is determined by the voxel size. Voxel size equals pixel size multiplied by level thickness, pixel size is determined by FOV and matrix (35). When the FOV is constant, the larger the matrix, the smaller the pixel; the smaller the FOV when the matrix remains unchanged, the smaller the pixels. Therefore, the pixel size can be reduced by increasing the matrix and reducing the FOV. The smaller the pixels, the thinner the level thickness, the smaller the impact of the partial volume effect, the higher the image spatial resolution (36). By the method of reducing pixel and thin layer scanning, the spatial resolution of the image can be improved, but the corresponding image SNR decreases, and the scanning time is extended. Reduced FOV imaging technique with ZOOM-EPI significantly improves image spatial resolution by reducing voxel (12,24).

Selection of the b values

The concept of the b value is the strength of the diffusion-sensitive gradient. It is proportional to the amplitude of the gradient, the duration of the applied gradient, and the time interval between the paired gradient. The measurement unit is square mm per second (37). According to the intravoxel incoherent motion (IVIM) theory, DWI reflects both the simplicial diffusion motion of water molecules and the blood perfusion of microcirculation (38). At low b, the measured ADC value is high due to blood perfusion and other factors, while the b value is large, the resulting ADC value almost completely represents diffusion because the perfusion effect is offset by a large gradient (39). In female pelvic studies, no consensus on the best choice of b value combinations. The b value should be increased to obtain a more realistic ADC value without affecting the image diagnosis. Therefore, high b value (b=1,000 s/mm^2) was chosen for this study.

IQ analyses

The results showed that the images obtained with the r-FOV DWI sequence had significant advantages in terms of image anatomical detail, image sharpness, image geometric distortion, motion, and magnetic sensitivity artifacts, and lesion significance compared with the conventional c-FOV DWI sequence. The agreement between the two radiologists' evaluations was relatively reliable, and the subjective evaluation index of the r-FOV DWI sequence was higher than that of the c-FOV DWI sequence. Consistent with previous findings (11,13-25), the present study confirmed that r-FOV

DWI can reduce image artifacts and distortions, and tumor edges can be displayed more clearly and better IQ can be obtained.

Objective evaluation of IQ showed that there was no significant difference between r-FOV DWI and c-FOV DWI in the cervical cancer group. The reason may be that the factors affecting SNR include the number of incentives, layer thickness, matrix, FOV, acquisition bandwidth, etc. The r-FOV DWI sequence has a reduced FOV and increased layer thickness, but the excitation number increases accordingly, so there is no significant effect on SNR.

In reality, comparing the findings of r-FOV and T1 anatomical serial slice images for anatomical features is challenging since the resolution and SNR of T1WI and r-FOV cervix scans are different, and T1WI shows the isointense in cervical/cervical cancer. As a result, r-FOV DWI cannot replace T1WI in terms of anatomical detail, and it can only highlight early imaging alterations in cervical cancer from a microscopic perspective (by improving image spatial resolution) (14,40-43).

Quantitative IQ analyses

The results showed that the difference in the mean ADC values between r-FOV DWI and c-FOV DWI sequences were statistically significant. r-FOV DWI sequences had an ADC value of $(0.690\pm0.195)\times10^{-3}$ mm^2/s, which is significantly lower than that of the c-FOV DWI sequence. Although they were statistically different, the two measurements are very close (0.690, and 0.794, respectively). This may be due to the higher spatial resolution, better fat suppression effects, and less motion, magnetic-sensitive artifacts, and reduces effect of microcirculatory perfusion, the measured ADC values are therefore more accurate. This result is not contradictory to the findings of other scholars. For example, Xing *et al.* (44) showed that in addition to having great diagnostic accuracy for measuring tumour invasion and MRI-T staging for esophageal cancer, high-resolution T2WI was able to distinguish clearly between normal and abnormal esophageal wall layers. Vidiri *et al.* (16) argue that head and neck tumors measured in r-FOV DWI sequence are lower and more accurate; Lu *et al.* (25) also found that the ADC measured by r-FOV DWI sequence in thyroid dispersion weighted imaging was lower than c-FOV DWI. However, Le Bihan *et al.* (38) indicated that there is no statistical difference in the ADC value of the two sequences in the pancreas; Zaharchuk *et al.* (45) showed no significant difference in human spinal cord ADC values in r-FOV DWI and c-FOV DWI sequences.

Comparison of ADC values between cervical cancer and normal cervix on r-FOV DWI sequences showed significantly different results. The ADC value of cervical cancer lesions was significantly lower than those of the normal cervix, indicating that the r-FOV DWI sequence has an important clinical value for the diagnosis of cervical cancer.

The ADC value has been studied in relation to cancer aggressiveness and is said to be linked to prognosis. Because of their enhanced cellularity and restricted water transport, ADC levels are lower in high-grade tumors (46). Somoye *et al.* (47) found that median mid-treatment ADC values were greater in survivors $(1.55\times10^3$ $mm^2/s)$ than in non-survivors $(1.36\times10^3$ $mm^2/s)$ among cervical cancer patients, with a 14% difference. ADC readings after four weeks of treatment are also said to be related to volume and clinical response (48). Patients that react to neoadjuvant chemotherapy have early increases in ADC values, which are negatively correlated with the proliferating cell nuclear antigen and cell density, demonstrating that ADC values are linked to cellular characteristics of the response that occur before size reduction (48).

Limitations of this study

Although this study objectively evaluated the clinical value of r-FOV DWI in terms of IQ, image SNR, CNR and ADC, the true clinical benefit of r-FOV has yet to be further demonstrated in future practice. The deficiencies of this paper also include: First, the relatively small number of patients in this study may have led to a selection bias for the different measurements. Second, patients should be instructed to fast for at least 6 to 8 hours prior to the MRI in order to reduce bowel peristalsis, and they may also receive anti-peristaltic medications (such as 20 mg of hyoscine butyl bromide or 1 mg of glucagon via intramuscular or intravenous injection) right before the exam to reduce severe image distortion caused by bowel contents (49,50). Third, only one level of the tumor region was selected for measurement in the ROI mapping, although three ROIs were randomly selected averaging, they did not reflect the overall tumor situation, the complete tumor volume measurement should be considered to ensure the accuracy and authenticity of the measurement. Fourth, the reduction of the imaging voxel increased the scanning time while improving the spatial resolution, and the next step should be to further optimize the sequence parameters and appropriately shorten the scanning time while ensuring the image SNR and spatial resolution.

Conclusions

r-FOV DWI can significantly improve image spatial resolution while reducing distortion and artifacts. Furthermore, more realistic ADC readings can aid in the more accurate diagnosis of cervical cancer.

Acknowledgments

Funding: None.

Footnote

Conflicts of Interest: All authors have completed the ICMJE uniform disclosure form (available at https://qims.amegroups.com/article/view/10.21037/qims-22-579/coif). The authors have no conflicts of interest to declare.

Ethical Statement: The authors are accountable for all aspects of the work in ensuring that questions related to the accuracy or integrity of any part of the work are appropriately investigated and resolved. The study was conducted in accordance with the Declaration of Helsinki (as revised in 2013). This study was approved by the Ethics Committee of Sun Yat-sen University (ID of the approval: 2020-536). All patients signed an informed consent form before the MR examination was performed. Informed consent was obtained from each patient for this study analysis.

References

1. Tsikouras P, Zervoudis S, Manav B, Tomara E, Iatrakis G, Romanidis C, Bothou A, Galazios G. Cervical cancer: screening, diagnosis and staging. J BUON 2016;21:320-5.
2. Ginsburg O, Bray F, Coleman MP, Vanderpuye V, Eniu A, Kotha SR, et al. The global burden of women's cancers: a grand challenge in global health. Lancet 2017;389:847-60.
3. Lee SI, Atri M. 2018 FIGO Staging System for Uterine Cervical Cancer: Enter Cross-sectional Imaging. Radiology 2019;292:15-24.
4. Koh DM, Collins DJ. Diffusion-weighted MRI in the body: applications and challenges in oncology. AJR Am J Roentgenol 2007;188:1622-35.
5. Pagani E, Bizzi A, Di Salle F, De Stefano N, Filippi M. Basic concepts of advanced MRI techniques. Neurol Sci 2008;29 Suppl 3:290-5.
6. Morelli J, Porter D, Ai F, Gerdes C, Saettele M, Feiweier T, Padua A, Dix J, Marra M, Rangaswamy R, Runge V. Clinical evaluation of single-shot and readout-segmented diffusion-weighted imaging in stroke patients at 3 T. Acta Radiol 2013;54:299-306.
7. Hu J, Li M, Dai Y, Geng C, Tong B, Zhou Z, Liang X, Yang W, Zhang B. Combining SENSE and reduced field-of-view for high-resolution diffusion weighted magnetic resonance imaging. Biomed Eng Online 2018;17:77.
8. Zhong Z, Merkitch D, Karaman MM, Zhang J, Sui Y, Goldman JG, Zhou XJ. High-Spatial-Resolution Diffusion MRI in Parkinson Disease: Lateral Asymmetry of the Substantia Nigra. Radiology 2019;291:149-57.
9. Xu C, Sun H, Xu Y, Wang W. Progress of MR reduced field-of-view dispersion weighted imaging in imaging diagnosis. Nuclear Magnetic Resonance 2017;8:556-60.
10. Wheeler-Kingshott CA, Parker GJ, Symms MR, Hickman SJ, Tofts PS, Miller DH, Barker GJ. ADC mapping of the human optic nerve: increased resolution, coverage, and reliability with CSF-suppressed ZOOM-EPI. Magn Reson Med 2002;47:24-31.
11. He YL, Hausmann D, Morelli JN, Attenberger UI, Schoenberg SO, Riffel P. Renal zoomed EPI-DWI with spatially-selective radiofrequency excitation pulses in two dimensions. Eur J Radiol 2016;85:1773-7.
12. Attenberger UI, Tavakoli A, Stocker D, Stieb S, Riesterer O, Turina M, Schoenberg SO, Pilz L, Reiner CS. Reduced and standard field-of-view diffusion weighted imaging in patients with rectal cancer at 3 T-Comparison of image quality and apparent diffusion coefficient measurements. Eur J Radiol 2020;131:109257.
13. Seeger A, Klose U, Bischof F, Strobel J, Ernemann U, Hauser TK. Zoomed EPI DWI of Acute Spinal Ischemia Using a Parallel Transmission System. Clin Neuroradiol 2016;26:177-82.
14. von Morze C, Kelley DA, Shepherd TM, Banerjee S, Xu D, Hess CP. Reduced field-of-view diffusion-weighted imaging of the brain at 7 T. Magn Reson Imaging 2010;28:1541-5.
15. Seeger A, Schulze M, Schuettauf F, Ernemann U, Hauser TK. Advanced diffusion-weighted imaging in patients with optic neuritis deficit - value of reduced field of view DWI and readout-segmented DWI. Neuroradiol J 2018;31:126-32.
16. Vidiri A, Minosse S, Piludu F, Curione D, Pichi B, Spriano G, Marzi S. Feasibility study of reduced field of view diffusion-weighted magnetic resonance imaging in head and neck tumors. Acta Radiol 2017;58:292-300.
17. Tamada T, Ream JM, Doshi AM, Taneja SS, Rosenkrantz AB. Reduced Field-of-View Diffusion-Weighted Magnetic Resonance Imaging of the Prostate at 3 Tesla: Comparison With Standard Echo-Planar Imaging Technique for Image Quality and Tumor Assessment. J Comput Assist Tomogr 2017;41:949-56.
18. Thierfelder KM, Sommer WH, Dietrich O, Meinel FG, Theisen D, Paprottka PM, Strobl FF, Pfeuffer J, Reiser MF, Nikolaou K. Parallel-transmit-accelerated

spatially-selective excitation MRI for reduced-FOV diffusion-weighted-imaging of the pancreas. Eur J Radiol 2014;83:1709-14.
19. Kim H, Lee JM, Yoon JH, Jang JY, Kim SW, Ryu JK, Kannengiesser S, Han JK, Choi BI. Reduced Field-of-View Diffusion-Weighted Magnetic Resonance Imaging of the Pancreas: Comparison with Conventional Single-Shot Echo-Planar Imaging. Korean J Radiol 2015;16:1216-25.
20. Hwang J, Hong SS, Kim HJ, Chang YW, Nam BD, Oh E, Lee E, Cha H. Reduced field-of-view diffusion-weighted MRI in patients with cervical cancer. Br J Radiol 2018;91:20170864.
21. Takeuchi M, Matsuzaki K, Bando Y, Harada M. Reduced field-of-view diffusion-weighted MR imaging for assessing the local extent of uterine cervical cancer. Acta Radiol 2020;61:267-75.
22. Deng B, Li Z, Hu D, Wang Y, Wu S. Clinical value of reduced field-of view diffusion weighted imaging in cervical cancer. Nuclear Magnetic Resonance 2020;11:487-92.
23. Cho E, Lee JH, Baek HJ, Ha JY, Ryu KH, Park SE, Moon JI, Gho SM, Wakayama T. Clinical Feasibility of Reduced Field-of-View Diffusion-Weighted Magnetic Resonance Imaging with Computed Diffusion-Weighted Imaging Technique in Breast Cancer Patients. Diagnostics (Basel) 2020.
24. Peng Y, Li Z, Tang H, Wang Y, Hu X, Shen Y, Hu D. Comparison of reduced field-of-view diffusion-weighted imaging (DWI) and conventional DWI techniques in the assessment of rectal carcinoma at 3.0T: Image quality and histological T staging. J Magn Reson Imaging 2018;47:967-75.
25. Lu Y, Hatzoglou V, Banerjee S, Stambuk HE, Gonen M, Shankaranarayanan A, Mazaheri Y, Deasy JO, Shaha AR, Tuttle RM, Shukla-Dave A. Repeatability Investigation of Reduced Field-of-View Diffusion-Weighted Magnetic Resonance Imaging on Thyroid Glands. J Comput Assist Tomogr 2015;39:334-9.
26. Janicek MF, Averette HE. Cervical cancer: prevention, diagnosis, and therapeutics. CA Cancer J Clin 2001;51:92-114; quiz 115-8.
27. Bhatla N, Berek JS, Cuello Fredes M, Denny LA, Grenman S, Karunaratne K, et al. Revised FIGO staging for carcinoma of the cervix uteri. Int J Gynaecol Obstet 2019;145:129-35.
28. Hricak H, Gatsonis C, Chi DS, Amendola MA, Brandt K, Schwartz LH, Koelliker S, Siegelman ES, Brown JJ, McGhee RB Jr, Iyer R, Vitellas KM, Snyder B, Long HJ 3rd, Fiorica JV, Mitchell DG; American College of Radiology Imaging Network 6651; Gynecologic Oncology Group 183. Role of imaging in pretreatment evaluation of early invasive cervical cancer: results of the intergroup study American College of Radiology Imaging Network 6651-Gynecologic Oncology Group 183. J Clin Oncol 2005;23:9329-37.
29. Merz J, Bossart M, Bamberg F, Eisenblaetter M. Revised FIGO Staging for Cervical Cancer - A New Role for MRI. Rofo 2020;192:937-44.
30. Cohen PA, Jhingran A, Oaknin A, Denny L. Cervical cancer. Lancet 2019;393:169-82.
31. Wang T, Gao T, Guo H, Wang Y, Zhou X, Tian J, Huang L, Zhang M. Preoperative prediction of parametrial invasion in early-stage cervical cancer with MRI-based radiomics nomogram. Eur Radiol 2020;30:3585-93.
32. Takeuchi M, Matsuzaki K, Harada M. The feasibility of reduced field-of-view diffusion-weighted imaging in evaluating bladder invasion of uterine cervical cancer. Br J Radiol 2022;95:20210692.
33. Chen M, Feng C, Wang Q, Li J, Wu S, Hu D, Deng B, Li Z. Comparison of reduced field-of-view diffusion-weighted imaging (DWI) and conventional DWI techniques in the assessment of Cervical carcinoma at 3.0T: Image quality and FIGO staging. Eur J Radiol 2021;137:109557.
34. Yang Z, Feng F, Wang X. Magnetic resonance Imaging Technical Guidelines - Inspection Specification, Clinical Strategies and New Technologies (Revised). June, 2007 1st Edition - Beijing: The People's Military Medical Publishing House, 2007:1-816.
35. Piccini D, Demesmaeker R, Heerfordt J, Yerly J, Di Sopra L, Masci PG, Schwitter J, Van De Ville D, Richiardi J, Kober T, Stuber M. Deep Learning to Automate Reference-Free Image Quality Assessment of Whole-Heart MR Images. Radiol Artif Intell 2020;2:e190123.
36. Meixner M, Foerst P, Windt CW. Reduced spatial resolution MRI suffices to image and quantify drought induced embolism formation in trees. Plant Methods 2021;17:38.
37. Qayyum A. Diffusion-weighted imaging in the abdomen and pelvis: concepts and applications. Radiographics 2009;29:1797-810.
38. Le Bihan D, Breton E, Lallemand D, Aubin ML, Vignaud J, Laval-Jeantet M. Separation of diffusion and perfusion in intravoxel incoherent motion MR imaging. Radiology 1988;168:497-505.
39. Yamada I, Aung W, Himeno Y, Nakagawa T, Shibuya H. Diffusion coefficients in abdominal organs and hepatic

lesions: evaluation with intravoxel incoherent motion echo-planar MR imaging. Radiology 1999;210:617-23.
40. Lam WW, So NM, Yang WT, Metreweli C. Detection of parametrial invasion in cervical carcinoma: role of short tau inversion recovery sequence. Clin Radiol 2000;55:702-7.
41. Kuroki Y, Nasu K. Advances in breast MRI: diffusion-weighted imaging of the breast. Breast Cancer 2008;15:212-7.
42. Zaspel U, Hamm B. Cervical cancer. In: Forstner R, Cunha TM, Hamm B. editors. MRI and CT of the female pelvis. Springer, 2017:121-80.
43. Padhani AR, Liu G, Koh DM, Chenevert TL, Thoeny HC, Takahara T, Dzik-Jurasz A, Ross BD, Van Cauteren M, Collins D, Hammoud DA, Rustin GJ, Taouli B, Choyke PL. Diffusion-weighted magnetic resonance imaging as a cancer biomarker: consensus and recommendations. Neoplasia 2009;11:102-25.
44. Xing X, Kuang X, Li X, Cheng Y, Liu F. Potential use of high-resolution T2-weighted MRI with histopathologic findings in staging esophageal cancer. Quant Imaging Med Surg 2023;13:249-58.
45. Zaharchuk G, Saritas EU, Andre JB, Chin CT, Rosenberg J, Brosnan TJ, Shankaranarayan A, Nishimura DG, Fischbein NJ. Reduced field-of-view diffusion imaging of the human spinal cord: comparison with conventional single-shot echo-planar imaging. AJNR Am J Neuroradiol 2011;32:813-20.
46. Otero-García MM, Mesa-Álvarez A, Nikolic O, Blanco-Lobato P, Basta-Nikolic M, de Llano-Ortega RM, Paredes-Velázquez L, Nikolic N, Szewczyk-Bieda M. Role of MRI in staging and follow-up of endometrial and cervical cancer: pitfalls and mimickers. Insights Imaging 2019;10:19.
47. Somoye G, Harry V, Semple S, Plataniotis G, Scott N, Gilbert FJ, Parkin D. Early diffusion weighted magnetic resonance imaging can predict survival in women with locally advanced cancer of the cervix treated with combined chemo-radiation. Eur Radiol 2012;22:2319-27.
48. Fu C, Feng X, Bian D, Zhao Y, Fang X, Du W, Wang L, Wang X. Simultaneous changes of magnetic resonance diffusion-weighted imaging and pathological microstructure in locally advanced cervical cancer caused by neoadjuvant chemotherapy. J Magn Reson Imaging 2015;42:427-35.
49. Abdulaal OM, MacMahon PJ, Rainford L, Cradock A, O'Driscoll D, Galligan M, Alshoabi SA, Alsharif W, McGee A. Evaluation of image quality of diffusion weighted readout segmentation of long variable echo-trains MR pulse sequence for lumbosacral nerve imaging at 3T. Quant Imaging Med Surg 2023;13:196-209.
50. Balleyguier C, Sala E, Da Cunha T, Bergman A, Brkljacic B, Danza F, Forstner R, Hamm B, Kubik-Huch R, Lopez C, Manfredi R, McHugo J, Oleaga L, Togashi K, Kinkel K. Staging of uterine cervical cancer with MRI: guidelines of the European Society of Urogenital Radiology. Eur Radiol 2011;21:1102-10.

Cite this article as: Mao L, Zhang X, Chen T, Li Z, Yang J. High-resolution reduced field-of-view diffusion-weighted magnetic resonance imaging in the diagnosis of cervical cancer. Quant Imaging Med Surg 2023;13(6):3464-3476. doi: 10.21037/qims-22-579

